

Anticrossing process in the vibronic relaxation of F centers in KClNorio Akiyama¹ and Shinji Muramatsu²¹*Department of Electronic Engineering, Okayama University of Science, Okayama 700-0005, Japan*²*Department of Electrical and Electronic Engineering, Utsunomiya University, Utsunomiya 321-8585, Japan*

(Received 19 July 2002; revised manuscript received 25 October 2002; published 19 March 2003)

The deexcitation process of F centers in KCl has been investigated by means of hot luminescence spectra measured with time-resolved spectroscopy under one-photon and two-photon excitation. An analysis of the experimental results was performed by considering the vibronic mixing of $2s$ and $2p$ excited states. From this analysis, it was found that the deexcitation after one (two) -photon excitation does not proceed along the zero-order potential energy surface (PES) of the $2p$ ($2s$) state which crosses the PES of the $2s(2p)$ state, but proceeds along one of the PES's that are obtained after $2s$ - $2p$ mixing interaction is included. By using the present results and other existing data on the F centers in KCl, a brief sketch of the potential energy curves is given.

DOI: 10.1103/PhysRevB.67.125115

PACS number(s): 78.47.+p, 61.72.Ji, 63.20.Kr

I. INTRODUCTION

The recent development of time-resolved spectroscopy techniques has made it possible to clarify the dynamical aspect of the deexcitation of electrons in molecules and clusters and self-trapped excitons in insulators after optical excitation.¹⁻³ In the F center in alkali halides, which is a typical example of a strongly coupled electron-lattice system and is also the simplest point defect in crystals,^{4,5} sophisticated femtosecond pump-probe optical-absorption experiments have been performed by Scholz *et al.*⁶ and an aspect of the lattice relaxation in the early time region after optical excitation has been revealed. However, the fundamental process of the lattice relaxation from absorption to emission in the F center has yet to be described completely.

The optical pumping process of F centers consists of the following three components. First, resonant Raman scattering (RRS) appears immediately after optical excitation from the ground state (g.s.) to the Franck-Condon state (FCS) which is the final state in absorption. Next, subsequent ultrafast relaxation is accompanied by a weak ultrafast emission [hot luminescence (HL)] during relaxation from the FCS to the relaxed excited state (RES). The final process is the return of the electron to the GS through ordinary luminescence (OL) from the RES. These components are correlated with each other and the whole process involving the RRS, HL, and OL is called the resonant secondary radiation (RSR).^{7,8} Interestingly, in F centers such as those in NaI and LiF a nonradiative process occurs with a little or no luminescence even at liquid helium temperature. Dexter, Klick, and Russell (DKR) criterion⁹ for such a nonradiative process has been established.¹⁰⁻¹³

The electronic state of the F center in the FCS and RES has been extensively studied by experiments using external perturbations (Stark, stress, magnetic effects), Raman scattering,¹⁴ optical detection of the magnetic resonance, and also by theoretical investigations¹⁵⁻²¹ that analyze these experimental data. Examples of the quantities extracted from these investigations are the energy of $2s$ - $2p$ level splitting,^{22,23} electron-phonon interaction constants,²⁴⁻²⁶ the effective frequency of coupled phonons,²⁷⁻²⁹ spin-orbit interaction constants,³⁰⁻³² the $2p$ and $2s$ orbital radius,³³⁻³⁶

spin-mixing parameters,^{37,38} and spin-lattice relaxation time.^{31,39,40} According to these studies, the FCS is described as nearly pure $2p$ states, while the RES is described as a $2s$ state admixed with $2p$ states, called a $2s$ -like state. The Stark effect experiment shows that the $2s$ state is higher than the $2p$ states in the FCS,²² while they are inverted in the RES.²³ This indicates the presence of $2s$ - $2p$ level crossing between the FCS and RES,⁴¹ so that a dynamic nonradiative transition may occur between $2s$ and $2p$ states.⁴²

In order to detect the presence of a $2s$ - $2p$ level crossing in the relaxation process, it is necessary to measure the RSR spectrum over the whole Stokes range. Up to date, the RSR has been measured under one-photon excitation (OPE) giving rise to a $1s$ - $2p$ transition⁴³⁻⁴⁸ and under the two-photon excitation (TPE) leading to a $1s$ - $2s$ transition.⁴⁹⁻⁵² An experimental study using the TPE technique was first performed by Martini *et al.*⁴⁹ They observed an OL spectrum in which the peak shifted from that observed under the OPE to a higher energy, and found that its decay time was about half that in the OPE. They explained these observations on the basis of an anticrossing mixing process of the $2s$ and $2p$ states. Several years later, Vogler⁵⁰ measured the decay time of emission due to the TPE and reported that it did not change from that in the OPE. Casalboni *et al.*⁵¹ and Hanzawa *et al.*⁵² also tried to investigate the emission under the TPE, but did not observe the emission in the OL region. This problem has still not been settled.

Analysis of the RSR spectra for the OPE has been performed on the basis of the simplifying assumption that the F center is a two-level system consisting of $1s$ ground and $2p$ excited states for a localized F electron coupled with lattice vibrations.^{7,42,48,53-57} Nevertheless, still now accepted understanding for a role of the $2s$ - $2p$ level crossing in the relaxation process in F centers has not been established. At present, the deexcitation process for the OPE is known to proceed as follows: It starts from the FCS (nearly pure $2p$ states), passes the level crossing point of $2s$ and $2p$ states without suffering from the effect of the $2s$ state during the vibronic relaxation and reaches a $2p$ -like state ($2p$ states admixed with $2s$ state), and finally goes to the $2s$ -like state, from which the OL occurs, through another level crossing

point located at the opposite side.⁴⁷ We have pointed out in a previous paper⁴⁸ that the presence of the $2s$ state cannot be neglected in the analysis of the deexcitation process.

The purpose of the present paper is to show how the $2s$ - $2p$ level crossing acts on the deexcitation process of the F center in KCl. We have performed a careful measurement of the RSR spectra for F centers in KCl under the OPE and TPE. The reason why we use the F center in KCl crystal is that the optical excitation to the $2s$ and $2p$ excited states in this center can be easily carried out. An attempt is made to explain these experimental results consistently by improving on the method used in our previous paper⁴⁸ to analyze the experimental result for the OPE. The present analysis is partly based on a model proposed by Bogan and Fitchen²³ for the RES. In Bogan and Fitchen's model, a pseudo-Jahn-Teller system of $2s$ and $2p$ states is treated phenomenologically by introducing a mixing parameter α by which $2s$ and $2p$ states are mixed. We assume that this mixing is realized not only in the RES but also during the relaxation. Therefore, the mixing parameter changes depending on the progress of the relaxation. This idea is incorporated into our previous treatment based on a time-resolved RSR spectrum under a pulse excitation formulated by Hama and Aihara⁵⁷ for a two level system such as a $1s$ - $2p$ one. We obtain the dependence of α on the wave number of emitted light from the experimental data for the OPE, and then use the obtained α to reproduce the experimental result for the TPE. We show that if the deexcitation is assumed to proceed, through the anti-crossing mixing process, from the $2p$ state to the $2s$ -like state under the OPE and from the $2s$ state to the $2p$ -like state under the TPE, experimental results for the OPE and TPE are consistently well explained.

II. EXPERIMENTS AND RESULTS

We used an additive colored crystal with F concentration N_F of $1.6 \times 10^{16} \text{ cm}^{-3}$. In the experiment for the OPE, an excitation light pulse from a cavity dumped dye laser (Coherent Antares 7220&702, dye: Rhodamine 6G, pulse duration ~ 8 ps, tuning range 16260 – 17730 cm^{-1}) excited by the second harmonics of the Nd^{3+} :YAG laser (Coherent Antares 76 s) was used. The repetition frequency of the excitation light pulse was 250 kHz. In the experiment for TPE, a mode-locked Q -switch YAG laser (9398 cm^{-1} , Q -switch pulse duration ~ 430 ns, mode-locked pulse duration ~ 80 ps) was used and the repetition frequency set to 2 kHz. Therefore, time-resolved measurements are possible not only in the μs -time region where a usual Q -switch pulse can be observed but also in the ps-time region where a mode-locked pulse constituting the Q -switch pulse can be observed. The energy of the fundamental light of the laser amounts to a half of the energy difference between $1s$ and $2s$ states of the F center in KCl. Moreover, we carried out the measurement carefully using a weak excitation power so as to avoid interactions between F centers induced by high power excitation. The RSR spectra from samples of KCl were measured with a streak scope (Hamamatsu C4334, absolute time-resolution ~ 15 ps, relative resolution ~ 2.6 ps) below 77 K (Oxford Microstat He) in both the experiments.

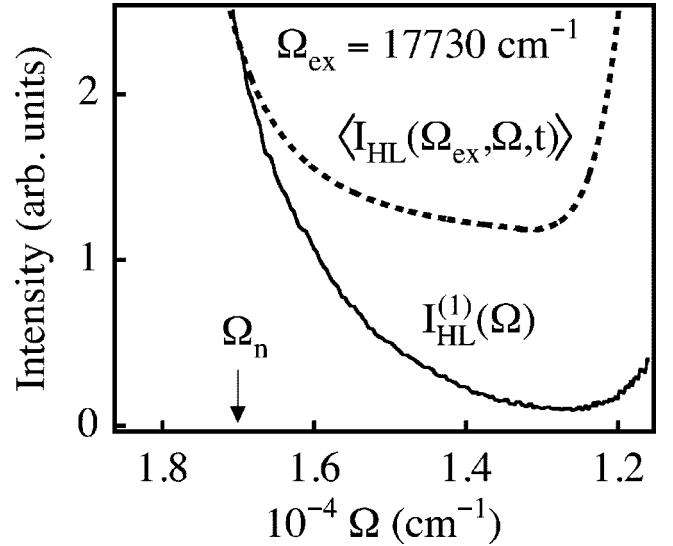


FIG. 1. The HL spectrum $I_{\text{HL}}^{(1)}(\Omega)$ measured under the OPE (excitation energy $\Omega_{\text{ex}} = 17730 \text{ cm}^{-1}$) is shown along with the calculated spectrum $\langle I_{\text{HL}}(\Omega_{\text{ex}}, \Omega, t) \rangle$.

In Fig. 1, a typical HL spectrum $I_{\text{HL}}^{(1)}(\Omega)$ for the OPE, which is compensated by Ω^3 , is shown as a function of the wave number of emitted light Ω . This was obtained from the time-resolved RSR spectrum for the OPE, using a method described in our previous paper.⁴⁸ The $I_{\text{HL}}^{(1)}(\Omega)$ monotonously decreases with decreasing Ω down to near 12500 cm^{-1} , but then increases as Ω further decreases in our experimental range. We have pointed out that the rise of the HL is due to the oscillation of the phonon wave packet during relaxation around the thermal equilibrium point, where the OL takes place.⁴⁸

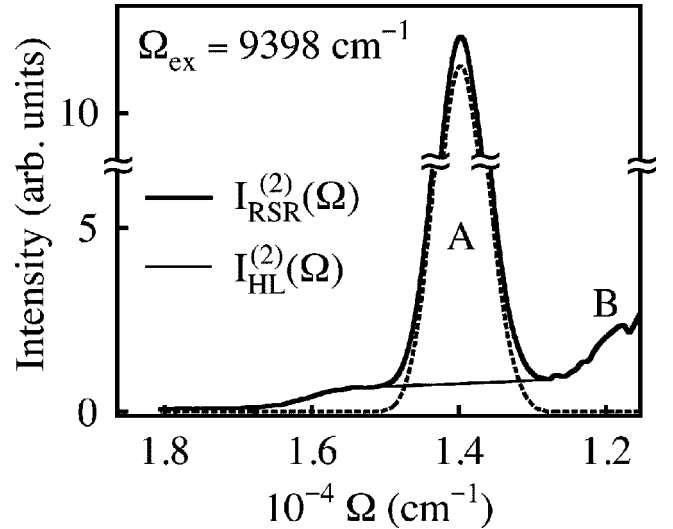


FIG. 2. The RSR spectrum $I_{\text{RSR}}^{(2)}(\Omega)$ for the TPE (excitation energy $\Omega_{\text{ex}} = 9398 \text{ cm}^{-1}$), which is compensated by Ω^3 , is shown by a solid line composed of two components. One (A band) is attributed to an aggregation of complex F centers, and the other [$I_{\text{HL}}^{(2)}(\Omega)$] is the HL component in which we are interested.

A typical observed RSR spectrum $I_{\text{RSR}}^{(2)}(\Omega)$ for the TPE, which is compensated by Ω^3 , is shown in Fig. 2. In this spectrum for the TPE, the RSR spectrum intensity increases with decreasing Ω in contrast to that for OPE in Fig. 1. We consider that the RSR spectrum from 18 000 to 15 000 cm^{-1} has only the HL component, as in the case of the OPE, because it shows emission having the same time width as the mode-locked pulse of 80 ps. In addition, the RSR for the TPE has a large emission band at about 14 000 cm^{-1} , and a weak emission band around 12 000 cm^{-1} . We call these bands *A*- and *B*- emission bands, respectively. The intensity of these emission bands is nearly proportional to the square of the excitation power, when the excitation density is between 1.1×10^4 to 1.6×10^5 W cm^{-2} . This means that there are emission due to the TPE. Casalboni *et al.*⁵¹ and Hanzawa *et al.*⁵² have already observed the *A*-emission band at 14 000 cm^{-1} . Casalboni *et al.*⁵¹ reported that its intensity increases as the third power of the incident laser power. However, our result corresponds with the second power dependence, and is the same as that obtained by Hanzawa *et al.*⁵² The other bands observed by Casalboni *et al.*⁵¹ have not been found in our experiment. We first measured the radiative lifetime of the *A*-emission band and determined it to be 7 ns from a single exponential decay. The origin of this band has been attributed to an aggregation of complex *F* centers (*F*₂ centers)⁵¹ or to a loose couple of *F* centers,⁵² although a detailed explanation of this emission band has not yet been given.

On the other hand, the radiative lifetime of the weak *B*-emission band observed under the TPE around 12 100 cm^{-1} is 550 ns, which is the same as that of the OL observed under the OPE. This agrees with experimental result of Vogler,⁵⁰ but is not in agreement with the result of Martini *et al.*⁴⁹ who reported a difference between the radiative lifetimes of the OL under the OPE and TPE. We have also measured the emission near 12 100 cm^{-1} in the time region where the mode-locked pulse can be observed. The emission shows a fast decay of about 3 ns followed by a slow decay corresponding to the radiative lifetime of 550 ns.

The emission that slowly increases with decreasing Ω in Fig. 2, denoted by $I_{\text{HL}}^{(2)}(\Omega)$, has a short decay time equal to the duration time of the mode-locked pulse. Moreover, the shape of the emission spectrum is independent of N_F up to 4×10^{17} cm^{-3} . Therefore, $I_{\text{HL}}^{(2)}(\Omega)$ represents the HL spectrum due to the TPE.

III. ANALYSIS AND DISCUSSION

In this section, we analyze our experimental results taking into account the mixing effect of the *2s* and *2p* states. Our calculation relies on Eq. (9) in Ref. 57, which provides the time (*t*) resolved RSR spectrum under a pulse excitation and is given by

$$I_0(\Omega_{\text{ex}}, \Omega, t) = (2\pi)^2 \frac{\delta_0}{\sqrt{\pi}} I_a(\Omega_{\text{ex}}) \int_{-\infty}^{\infty} d\tau_0 \times e^{-\delta_0^2(\tau_0 - t)^2 - \gamma\tau_0} I_e(\Omega_{\text{ex}}, \Omega, \tau_0), \quad (1)$$

where $I_a(\Omega_{\text{ex}})$ denotes the normalized absorption spectrum, $I_e(\Omega_{\text{ex}}, \Omega, \tau_0)$ denotes the emission spectrum at time τ_0 , and both have a Gaussian form; Ω_{ex} and Ω denote the wave numbers of the exciting and detected photons, respectively, and δ_0 is a parameter which depends on the spectral width of the exciting pulse and the spectral resolution of the measurement system. The exponential factor of $-\gamma\tau_0$ denotes the radiative decay. The $I_e(\Omega_{\text{ex}}, \Omega, \tau_0)$ involves the spectral intensity $J(\omega)$, which represents the distribution of electron-phonon interaction intensity over the coupled phonon frequency ω . We use the following form similar to that proposed by Kayanuma,⁵⁶

$$J(\omega) = \begin{cases} \frac{16g\omega^2}{\pi C\omega_m^2} (\omega_m\omega - \omega^2)^{1/2}, & 0 \leq \omega < \omega_m, \\ 0, & \text{otherwise,} \end{cases} \quad (2)$$

where g is a dimensionless coupling constant, and ω_m the maximum phonon frequency, which is given by $C\bar{\omega}$,⁴⁸ $\bar{\omega}$ being an average phonon frequency. The $I_e(\Omega_{\text{ex}}, \Omega, \tau_0)$ also contains information about the time evolution of the phonon wave packet created by optical excitation.⁵⁷

In this paper, we are interested in analyzing the HL spectrum. It is important to note the following. Our experimental HL spectrum, obtained by using a convolution method, is integrated over the time range of the excitation light pulse. We denote the experimental HL spectrum by $I_{\text{HL}}^{(1)}(\Omega)$ for the OPE and $I_{\text{HL}}^{(2)}(\Omega)$ for the TPE. The measured spectra $I_{\text{HL}}^{(1)}(\Omega)$ and $I_{\text{HL}}^{(2)}(\Omega)$ do not directly correspond to the quantity given by Eq. (1), but to the time integrated HL spectrum over the time range of the excitation light pulse after subtracting the same time range of the OL component from $I_0(\Omega_{\text{ex}}, \Omega, t)$. Therefore, the time integrated HL spectrum $\langle I_{\text{HL}}(\Omega_{\text{ex}}, \Omega, t) \rangle$, which is to be compared with the measured spectrum $I_{\text{HL}}^{(1)}(\Omega)$ or $I_{\text{HL}}^{(2)}(\Omega)$, is given by

$$\langle I_{\text{HL}}(\Omega_{\text{ex}}, \Omega, t) \rangle = \langle I_0(\Omega_{\text{ex}}, \Omega, t) - I_{\text{OL}}(\Omega_{\text{ex}}, \Omega, t) \rangle, \quad (3)$$

where the second term corresponds to the build up spectrum of the OL component simulated by using Eq. (1).⁴⁸

We examined how the three parameters γ , g , and ω_m , affect the calculated HL spectrum for the OPE given by Eq. (3), by varying γ from $2.5 \times 10^{-5} \bar{\omega}$ to $2.5 \times 10^{-2} \bar{\omega}$, and also varying the values of ω_m and g . However, even when the best choice of the parameter value was achieved, the disagreement in the intensity seen in Fig. 1 was still observed.

Equation (1) has been derived under the assumption that the matrix element of the electric dipole moment between the initial and final states of emission is a constant and taken as unity. In order to take into account the mixing effect of the *2s* and *2p* states, as calculated HL spectrum we take the following equation:

$$I_{\text{HL}}(\Omega_{\text{ex}}, \Omega) = |M(\Omega)|^2 \langle I_{\text{HL}}(\Omega_{\text{ex}}, \Omega, t) \rangle, \quad (4)$$

where $M(\Omega)$ is the matrix element of the electric dipole moment of emission and assumed to be a function of Ω . The $M(\Omega)$ can be related to the Bogan and Fitchen's model,²³ if we assume that it holds not only in the RES but also during

the relaxation. According to this model, the $2s$ -like and $2p$ -like states take the following form:

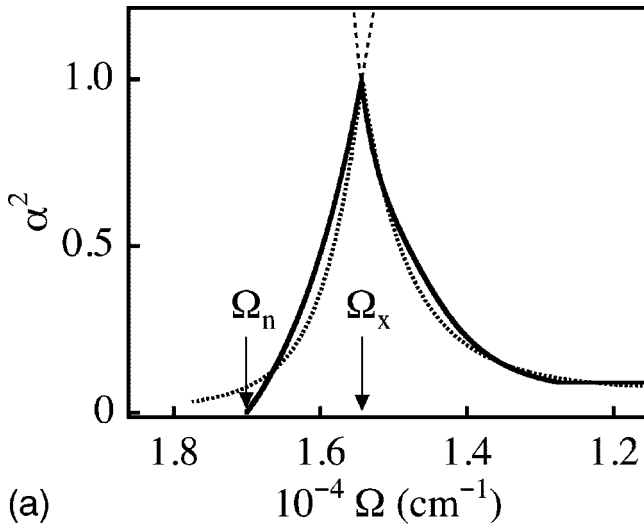
$$|2s'\rangle = \frac{1}{\sqrt{1+\alpha^2}}(|2s\rangle + \alpha|p\rangle), \quad (5)$$

$$|2p'\rangle = \frac{1}{\sqrt{1+\alpha^2}}(|p\rangle - \alpha|2s\rangle), \quad (6)$$

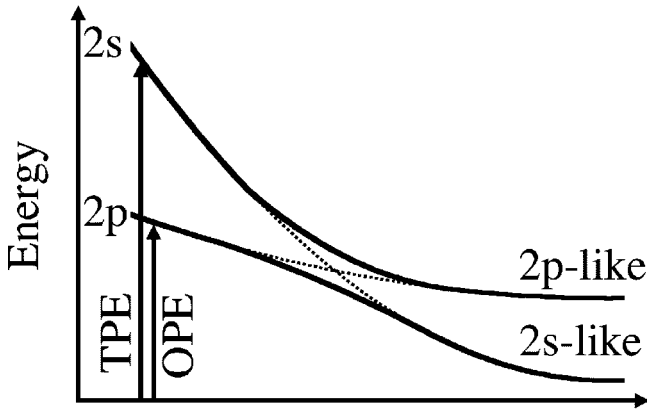
where α is a mixing parameter ranging from 0 to 1, and

$$|p\rangle = \frac{1}{\sqrt{b_1^2+b_2^2+b_3^2}}(b_1|2p_x\rangle + b_2|2p_y\rangle + b_3|2p_z\rangle). \quad (7)$$

We assume that α is a function of Ω . For the transition from the $2p$ -like state to the ground $1s$ state, $|M(\Omega)|^2$



(a)



(b) Configuration Coordinate

FIG. 3. (a) The value of α^2 obtained from the fitting of Eq. (12) to $I_{\text{HL}}^{(1)}(\Omega)$ shown in Fig. 1. The dotted curve is the value of α^2 obtained from a semiclassical calculation. For Ω_n and Ω_x see the text. (b) Potential energy surfaces are schematically shown for the OPE and TPE against a configuration coordinate along which vibrational relaxation proceeds. The dotted curves show the level crossing when the $2s$ - $2p$ mixing is ignored.

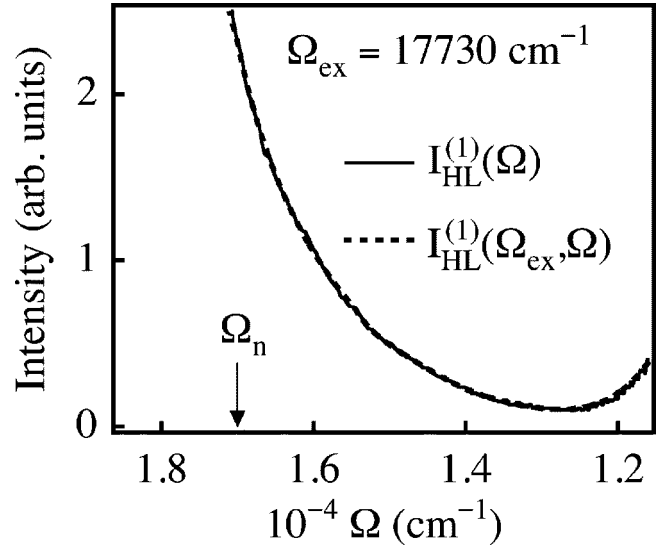


FIG. 4. Comparison of the calculated HL spectrum $I_{\text{HL}}^{(1)}(\Omega_{\text{ex}}, \Omega)$ for OPE with the measured spectrum $I_{\text{HL}}^{(1)}(\Omega)$.

$=|M_x|^2/(1+\alpha^2)$, and for the transition from the $2s$ -like state to the ground $1s$ state, $|M(\Omega)|^2 = |M_x|^2 \alpha^2 / (1+\alpha^2)$, where $|M_x|^2 = |\langle 1s|x|2p_x\rangle|^2$ if we assume that $|\langle 1s|x|2p_x\rangle|^2 = |\langle 1s|y|2p_y\rangle|^2 = |\langle 1s|z|2p_z\rangle|^2 = 1$. Hereafter, we denote the former and latter values of $|M(\Omega)|^2$ elements by $|M_{2p'}(\Omega)|^2$ and $|M_{2s'}(\Omega)|^2$, respectively. Therefore, the calculated HL spectrum is given by $I_{\text{HL}}(\Omega_{\text{ex}}, \Omega) = |M_{2p'}(\Omega)|^2 \langle I_{\text{HL}}(\Omega_{\text{ex}}, \Omega, t) \rangle$ if the emission takes place through the transition from the $2p$ -like state to the $1s$ state, or $I_{\text{HL}}(\Omega_{\text{ex}}, \Omega) = |M_{2s'}(\Omega)|^2 \langle I_{\text{HL}}(\Omega_{\text{ex}}, \Omega, t) \rangle$ if the emission occurs through the transition from the $2s$ -like state to the $1s$ state. It should be noted that when $\alpha=0$, $I_{\text{HL}}(\Omega_{\text{ex}}, \Omega) = \langle I_{\text{HL}}(\Omega_{\text{ex}}, \Omega, t) \rangle$, and corresponds to $\langle I_{\text{HL}} \rangle_{\text{sim}}$ in Ref. 48, where $I_{\text{HL}}^{(1)}(\Omega)$ is represented by $\langle I_{\text{HL}} \rangle_{\text{expt}} / \Omega^3$.

Setting $I_{\text{HL}}(\Omega_{\text{ex}}, \Omega) = |M_{2p'}(\Omega)|^2 \langle I_{\text{HL}}(\Omega_{\text{ex}}, \Omega, t) \rangle$ and comparing it to $I_{\text{HL}}^{(1)}(\Omega)$, we obtain the relation

$$\alpha^2 = \langle I_{\text{HL}}(\Omega_{\text{ex}}, \Omega, t) \rangle / I_{\text{HL}}^{(1)}(\Omega) - 1. \quad (8)$$

If we take $I_{\text{HL}}(\Omega_{\text{ex}}, \Omega) = |M_{2s'}(\Omega)|^2 \langle I_{\text{HL}}(\Omega_{\text{ex}}, \Omega, t) \rangle$, α^2 is determined as follows:

$$\alpha^2 = I_{\text{HL}}^{(1)}(\Omega) / [\langle I_{\text{HL}}(\Omega_{\text{ex}}, \Omega, t) \rangle - I_{\text{HL}}^{(1)}(\Omega)]. \quad (9)$$

We have obtained the value of α^2 from Eq. (8) as a function of Ω , using $I_{\text{HL}}^{(1)}(\Omega)$ and $\langle I_{\text{HL}}(\Omega_{\text{ex}}, \Omega, t) \rangle$ which was calculated with the optimum parameter values ($\gamma = 2.5 \times 10^{-5} \bar{\omega}$, $g = 40$, $C = 1.5$, and $\bar{\omega} = 110 \text{ cm}^{-1}$).⁴⁸ In the procedure for extracting the value of α^2 from experimental and calculated data, we normalized the magnitude of $\langle I_{\text{HL}}(\Omega_{\text{ex}}, \Omega, t) \rangle$ by the value of $I_{\text{HL}}^{(1)}(\Omega)$ at $\Omega_n = 17000 \text{ cm}^{-1}$ in Fig. 1. For $\Omega < \Omega_n$, the effect of the RRS can be regarded to be negligibly small. Thus, the obtained value of α^2 is plotted in Fig. 3(a), which shows that α^2 becomes larger than 1 for $\Omega < \Omega_x$ ($= 15430 \text{ cm}^{-1}$), as shown by the dashed curve. The Ω_x corresponds to the level crossing point of adiabatic potential energy surfaces for the $2s$ and $2p$ states, when the $2s$ - $2p$ mixing is neglected, because at the crossing

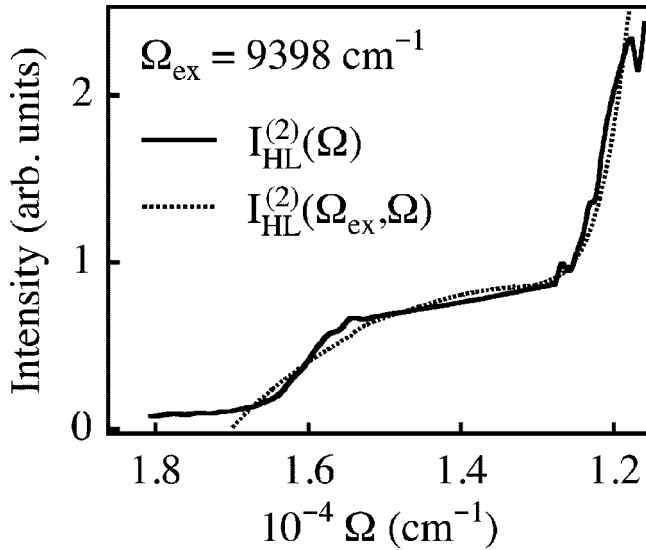


FIG. 5. Comparison of the calculated HL spectrum $I_{HL}^{(2)}(\Omega_{ex}, \Omega)$ for TPE with the measured spectrum $I_{HL}^{(2)}(\Omega)$.

point $\alpha=1$. In order to have the value of α^2 in a range between 0 and 1 for $\Omega < \Omega_x$, we have to use $I_{HL}(\Omega_{ex}, \Omega) = |M_{2s'}(\Omega)|^2 \langle I_{HL}(\Omega_{ex}, \Omega, t) \rangle$, and α^2 should be obtained from Eq. (9) rather than Eq. (8). The value of α^2 obtained from Eq. (9) is plotted in Fig. 3(a) as a solid curve for $\Omega < \Omega_x$. The entire curve of α^2 deduced from experimental data will be compared with the calculated result below.

From the above discussion, the spectrum of $I_{HL}(\Omega_{ex}, \Omega)$ for the OPE, $I_{HL}^{(1)}(\Omega_{ex}, \Omega)$, can be expressed as

$$I_{HL}^{(1)}(\Omega_{ex}, \Omega) = |M_{2p'}(\Omega)|^2 \langle I_{HL}(\Omega_{ex}, \Omega, t) \rangle \Theta(\Omega - \Omega_x) + |M_{2s'}(\Omega)|^2 \langle I_{HL}(\Omega_{ex}, \Omega, t) \rangle \times [1 - \Theta(\Omega - \Omega_x)], \quad (10)$$

where $\Theta(\Omega)$ is the step function. Equation (10) implies that the transfer from the $2p$ -like state to the $2s$ -like state occurs in the course of the relaxation as shown in Fig. 3(b). In Fig. 4 the $I_{HL}^{(1)}(\Omega)$ and its calculated spectrum given by Eq. (10) are compared. For $\Omega < \Omega_n$ they coincide well with each other. This is quite natural, since the value of α^2 is chosen so that the spectra agree.

We are now in a position to explain the experimental result of the TPE using the result of α^2 in Fig. 3(a). In this case $|M_{2p'}(\Omega)|^2$ and $|M_{2s'}(\Omega)|^2$ in Eq. (10) should be interchanged. Then, the expression for the TPE, $I_{HL}^{(2)}(\Omega_{ex}, \Omega)$, takes the following form:

$$I_{HL}^{(2)}(\Omega_{ex}, \Omega) = |M_{2s'}(\Omega)|^2 \langle I_{HL}(\Omega_{ex}, \Omega, t) \rangle \Theta(\Omega - \Omega_x) + |M_{2p'}(\Omega)|^2 \langle I_{HL}(\Omega_{ex}, \Omega, t) \rangle \times [1 - \Theta(\Omega - \Omega_x)]. \quad (11)$$

The calculated result using Eq. (11) is compared with the experimental result $I_{HL}^{(2)}$ in Fig. 5. They are in good agreement with each other, although we use α^2 in Fig. 3(a), which has been deduced from the experiment for the OPE. There-

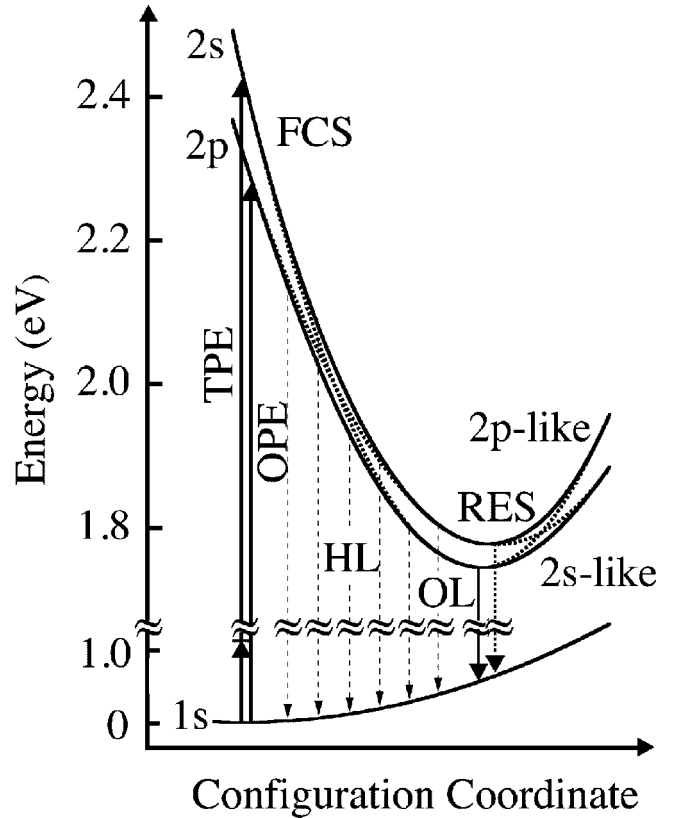


FIG. 6. Adiabatic potential energies of $2s$, $2p$, and $1s$ states, which are determined by using the present data for Ω_x and other data in the text. The OPE and TPE indicate one-photon excitation and two-photon excitation, respectively.

fore, we can say that if the mixing parameter α of the $2s$ and $2p$ states changes as shown in Fig. 3(a), our experimental results of the HL spectra for the OPE and TPE are described by Eqs. (10) and (11), respectively. Equation (10) implies the transfer from the $2p$ -like state to the $2s$ -like state, and Eq. (11) implies the transfer from the $2s$ -like state to the $2p$ -like state around the crossing point which would exist when $\alpha=0$, as shown in Fig. 3(b).

Here, we try to obtain the dependence of α^2 on Ω shown by the solid curve in Fig. 3(a) from a semiclassical calculation using existing data characterizing the F center in KCl. The relation between α^2 and Ω can be obtained by considering a 2×2 Hamiltonian matrix which has the following elements: $H_{11} = E_s(Q)$, $H_{22} = E_p(Q)$, and $H_{12} = H_{21}^* = V_{sp}$, where $E_s(Q)$ and $E_p(Q)$ denote adiabatic potential energy surfaces for the $2s$ and $2p$ states, respectively, as a function of the interaction coordinate Q along which the vibrational relaxation occurs, and V_{sp} is a constant parameter mixing those states. By getting eigenvectors of this matrix and comparing them with Eqs. (5) and (6), we obtain α^2 as

$$\alpha^2 = 2X^2 - 2|X| \sqrt{X^2 + 1} + 1, \quad (12)$$

where $X = [E_p(Q) - E_s(Q)] / |2V_{sp}|$. In order to calculate α^2 according to Eq. (12), we need to obtain $E_s(Q)$ and $E_p(Q)$, and furthermore the potential energy for the ground $1s$ state $E_g(Q)$ is required in order to relate α^2 to Ω , where Ω is

approximately given by $[E_p(Q) - E_g(Q)]/\hbar$ for $\Omega > \Omega_x$ and $[E_s(Q) - E_g(Q)]/\hbar$ for $\Omega < \Omega_x$. The $E_s(Q)$, $E_p(Q)$, and $E_g(Q)$ were determined by assuming a parabolic curvature and using the following six data: absorption (2.313 eV) and emission (1.174 eV) energies of the F band,⁴ energy differences between $2s$ and $2p$ states in the FCS (0.11 eV) (Ref. 58) and RES (0.0335 eV),¹⁸ lattice relaxation energy (0.569 eV) (Ref. 4), and Ω_x (1.913 eV = 15 430 cm^{-1}). The potentials are given in units of eV by $E_s(Q) = 1.19(Q - 0.7546)^2 + 1.7436$, $E_p(Q) = 0.804(Q - 0.8164)^2 + 1.7771$, and $E_g(Q) = Q^2$, and depicted in Fig. 6. In Fig. 6, we note that the curvatures at the bottom of new nonparabolic potentials, which are made from $E_s(Q)$ and $E_p(Q)$ by including the mixing interaction of the $2s$ and $2p$ states, are nearly the same. However, the coefficients of the quadratic terms of $E_s(Q)$ and $E_p(Q)$ are largely different, their ratio being 1.47. In Fig. 3(a), the α^2 is calculated by setting $V_{sp} = 0.013$ eV, and plotted against Ω as the dotted line, and is in good agreement with that deduced from experimental data of $I_{\text{HL}}^{(1)}(\Omega)$. It is important to note that in the results here α^2 has a constant value in the OL region. This is 0.08, which is somewhat smaller than the value of 0.15 found by Imanaka *et al.*¹⁸ from experiments on the Stark effect in the RES for the F center in KCl. The value of $V_{sp} = 0.013$ eV agrees well with the result of Iida *et al.*⁵⁹

We now make briefly discuss whether the obtained value of V_{sp} is suitable enough to support the anticrossing process. The $V_{sp} = 0.013$ eV (105 cm^{-1}) is nearly equal to the $\bar{\omega} = 110$ cm^{-1} used in the calculation of Eq. (3). According to Ref. 60, in which the $2s$ - $2p$ model calculation has been carried out for the transfer probability, this seems to be an adequate strength for the anticrossing process. We estimate the lattice relaxation time τ to be $\tau > 0.3$ ps, using $V_{sp} > h/\tau$.⁴⁹ On the other hand, Martini *et al.* obtained $\tau > 0.07$ ps. Our value of τ is about four times longer than that of Martini *et al.* However, it well corresponds to the result of our simulation for the dumping oscillation of the phonon wave packet as shown in Fig. 4(b) in Ref. 48. This good correspondence shows that our treatment is reasonable.

Martini *et al.*⁴⁹ presented a similar configuration coordinate diagram to Fig. 6 on the basis of their experimental observations, that is, different OL spectra from $2s$ - and $2p$ -like states with different lifetimes. Martini *et al.* have reported the OL arising from the $2p$ -like state. We also observe the OL in the TPE as described in Sec. II. Our measured radiative lifetime of the weak B -emission near 12 100 cm^{-1} in Fig. 2, which would correspond to the high-energy side of the OL band, is equal to that of the OL observed in the OPE within errors of measurement. However, this result does not necessarily imply that the OL under the TPE has originated from the $2s$ -like state. This is because in our scheme shown in Fig. 6 the OL may occur from the $2p$ -like state, as expected by assuming that the level anticrossing of the $2s$ - and $2p$ -like potentials occurs at the right hand side. Furthermore, we can suppose that the OL in the TPE arises from not only the $2p$ -like state but also the $2s$ -like state, provided that the mechanism of the deexcitation process around the anticrossing on the right hand side in

Fig. 6 is different from that at the left hand side. In this case, the OL would be composed of the emission from the $2s$ - and $2p$ -like states. On the other hand, the Bogan and Fitchen's model suggests that the radiative lifetime of the OL arising from the $2p$ -like state is α^2 times that from the $2s$ -like state. The former lifetime is estimated to be 44 ns (= 0.08×550 ns) by using the value of α^2 in Fig. 3(a). However, an emission with the expected lifetime of 44 ns was not observed. The observed emission is much faster with unexpected lifetime of only 3 ns. This seems to result from a stimulated emission due to 1.06 μm excitation, as suggested by Casalboni *et al.*⁵¹ We propose that electrons that do not suffer from the stimulated emission's effect could emit light from the $2s$ -like state with a radiative lifetime of 550 ns. From this, we infer that the emission observed in our experiment contains contributions from the $2p$ - and $2s$ -like states, since the population of the latter state is allowed by a tunneling effect between those states or due to an incomplete transfer⁶⁰ from the $2p$ -like to $2s$ -like state. Unfortunately, we could not observe the OL peaks because of the limitations of the detection sensitivity of our streak scope, and do not know whether the OL have different emission peaks or not. In order to verify the above picture for the OL in the TPE, we need to perform high sensitivity time-resolved measurements of the OL in the TPE.

Finally, we briefly discuss the experimental result of the depolarization spectrum in Fig. 3 in Ref. 48 in relation to our scheme. Experiments show that the degree of polarization of the HL does not vanish keeping a constant value until the OL region.⁴⁶⁻⁴⁸ In our scheme the polarization of the HL is governed by mixing coefficients b_1 , b_2 , and b_3 in Eq. (7), which are related to the coupling of the excited $2p$ states with t_{2g} modes. This vibronic coupling is switched on just when excitation occurs into the FCS. Namely, we suppose that the polarization of the HL is determined in the stage of RRS and remains roughly unchanged during the HL process where relaxation is caused by other modes than t_{2g} ones.^{24,26}

Experimental and theoretical studies on the dynamics in the early stage have been conducted by Sholtz *et al.*⁶ on the basis of the dynamical Jahn-Teller interactions of $2p$ states with e_{1g} and t_{2g} modes. Our understanding is in accord with the result of their investigation. Vanishing of the polarization in the OL region is probably due to thermalization in the RES, through vibronic coupling to t_{2g} modes with different coupling strengths²⁶ from that in the FCS.²⁴

IV. CONCLUSION

We have investigated the de-excitation process of F centers in KCl by measuring the HL spectra under the one-photon and two-photon excitation. We analyzed these experimental results taking into account the mixing effect of the $2s$ and $2p$ excited states. The mixing parameter α is determined from the HL spectrum for one-photon excitation as a function of the wave number of emitted light Ω . We have shown that the experimental HL spectrum under two-photon excitation can be reproduced well by using the determined parameter α . It is also shown that the dependence of α^2 on Ω can be well reproduced using the data obtained in the present

work and existing data characterizing the F center in KCl. Our value of α in the RES is consistent with that reported in the literature.

In conclusion, from measurements of the dynamical behavior of HL spectra for the F center in KCl, it is found that the vibronic relaxation follows an anticrossing process due to the interaction of the $2s$ and $2p$ excited states. In other words, one-photon excitation can proceed through the transfer from the $2p$ -like state to the $2s$ -like state, while two-

photon excitation can proceed through the transfer from the $2s$ -like state to the $2p$ -like state.

ACKNOWLEDGMENTS

The authors wish to thank Professor T. Iida of Osaka City University for valuable discussions and Dr. G. Baldacchini of ENEA (Italy) for continuing his deep interest in this work. We also thank Mr. A. Tsuchihashi and Mr. T. Kojo for their experimental help.

- ¹E. Schreiber, *Femtosecond Real-Time Spectroscopy of Small Molecules and Clusters*, Springer Tracts in Modern Physics Vol. 143 (Springer-Verlag, Berlin, 1998).
- ²K. S. Song and R. T. Williams, *Self-Trapped Excitons*, Springer Series in Solid State Sciences, Vol. 105 (Springer-Verlag, Berlin, 1993).
- ³S. Tomimoto, S. Saito, T. Suemoto, K. Sakata, J. Takeda, and S. Kurita, Phys. Rev. B **60**, 7961 (1999).
- ⁴See, e.g., *Physics of Color Centers*, edited by W. B. Fowler (Academic, New York, 1968), Chap. 2; *Electronic and Vibrational Properties of Point Defects in Ionic Crystals*, edited by Y. Farge and M. P. Fontana (North-Holland, Amsterdam, 1979), Chap. 4.
- ⁵G. Baldacchini, in *Optical Properties of Excited States in Solids*, edited by B. Di Bartolo (Plenum, New York, 1992), pp. 255–303.
- ⁶R. Scholz, M. Schreiber, F. Bassani, M. Nisoli, S. De Silvestri, and O. Svelto, Phys. Rev. B **56**, 1179 (1997).
- ⁷V. Hizhnyakov and I. Tehver, Phys. Status Solidi **21**, 755 (1967).
- ⁸Y. Toyozawa, J. Phys. Soc. Jpn. **41**, 400 (1976).
- ⁹D. L. Dexter, C. C. Klick, and G. A. Russell, Phys. Rev. **100**, 603 (1955).
- ¹⁰R. H. Bartram and A. M. Stoneham, Solid State Commun. **17**, 1593 (1975).
- ¹¹R. H. Bartram, J. Phys. Chem. Solids **51**, 641 (1990).
- ¹²G. Baldacchini, in *Advances in Nonradiative Processes in Solids*, edited by B. Di Bartolo (Plenum, New York, 1989), pp. 219–259.
- ¹³F. D. Matteis, M. Leblans, and D. Schoemaker, Phys. Rev. B **49**, 9357 (1994).
- ¹⁴D. S. Pan and F. Lüty, in *Light Scattering in Solids*, edited by M. Balkanski, R. C. C. Leite, and S. P. S. Port (Flammarion, Paris, 1975), p. 540.
- ¹⁵F. S. Ham, Phys. Rev. B **8**, 2926 (1973).
- ¹⁶F. S. Ham and U. Grevsmühl, Phys. Rev. B **8**, 2945 (1973).
- ¹⁷Y. Kayanuma, J. Phys. Soc. Jpn. **40**, 363 (1976).
- ¹⁸K. Imanaka, T. Iida, and H. Ohkura, J. Phys. Soc. Jpn. **43**, 519 (1977).
- ¹⁹K. Iwahana, T. Iida, and H. Ohkura, J. Phys. Soc. Jpn. **47**, 599 (1979).
- ²⁰J. Thomchick and F. S. Ham, Phys. Rev. B **22**, 6013 (1980).
- ²¹L. Martinelli, G. P. Parravicini, and O. L. Soriani, Phys. Rev. B **32**, 4106 (1985).
- ²²G. Chiarotti, U. M. Grassano, and R. Rosei, Phys. Rev. Lett. **17**, 1043 (1966).
- ²³L. D. Bogan and D. B. Fitchen, Phys. Rev. B **1**, 4122 (1970).
- ²⁴S. E. Schnatterly, Phys. Rev. **140**, A1364 (1965).
- ²⁵R. E. Hetrick and W. D. Compton, Phys. Rev. **155**, 649 (1967).
- ²⁶N. Akiyama, K. Asami, M. Ishiguro, and H. Ohkura, J. Phys. Soc. Jpn. **50**, 3427 (1981).
- ²⁷G. A. Russell and C. C. Klick, Phys. Rev. **101**, 1473 (1956).
- ²⁸F. Lüty and W. Gebhardt, Z. Phys. **169**, 475 (1962).
- ²⁹W. Gebhardt and H. Kuhnert, Phys. Status Solidi **14**, 157 (1966).
- ³⁰C. H. Henry, and C. P. Slichter, in *Physics of Color Centers*, edited by W. B. Fowler (Academic, New York, 1968), Chap. 6.
- ³¹G. Baldacchini, U. M. Grassano, and A. Tanga, Phys. Rev. B **19**, 1283 (1979).
- ³²H. Ohkura, K. Tara, N. Akiyama, K. Iwahana, and Y. Mori, J. Phys. Soc. Jpn. **51**, 3615 (1982).
- ³³H. Seidel and H. C. Wolf, in *Physics of Color Centers*, edited by W. B. Fowler (Academic, New York, 1968), Chap. 8.
- ³⁴H. J. Reyher, K. Hahn, Th. Vetter, and A. Z. Winnacker, Z. Phys. B: Condens. Matter **33**, 357 (1967).
- ³⁵L. F. Mollenauer and G. Baldacchini, Phys. Rev. Lett. **29**, 465 (1972).
- ³⁶N. Akiyama and H. Ohkura, Phys. Rev. B **53**, 10 632 (1996).
- ³⁷A. Winnacker and L. F. Mollenauer, Phys. Rev. B **6**, 787 (1972).
- ³⁸S. Muramatsu, N. Akiyama, Y. Mori, and H. Ohkura, J. Phys. Soc. Jpn. **55**, 2811 (1986).
- ³⁹H. Panepucci and L. F. Mollenaure, Phys. Rev. **178**, 589 (1969).
- ⁴⁰N. Akiyama and H. Ohkura, Phys. Rev. B **40**, 3232 (1989).
- ⁴¹R. F. Wood and U. Öpik, Phys. Rev. **179**, 783 (1969).
- ⁴²S. Muramatsu and K. Nasu, J. Phys. C **18**, 3729 (1985).
- ⁴³Y. Mori, R. Hattori, and H. Ohkura, J. Phys. Soc. Jpn. **51**, 2713 (1982).
- ⁴⁴Y. Mori and H. Ohkura, J. Phys. Chem. Solids **51**, 663 (1990).
- ⁴⁵Y. Kondo, T. Noto, S. Sato, M. Hirai, and A. Nakamura, J. Lumin. **38**, 164 (1987).
- ⁴⁶N. Akiyama and H. Ohkura, J. Lumin. **60/61**, 713 (1994).
- ⁴⁷N. Akiyama, S. Muramatsu, S. Ide, and H. Ohkura, J. Lumin. **87-89**, 568 (2000).
- ⁴⁸N. Akiyama, S. Muramatsu, and A. Tsuchihashi, J. Phys. Soc. Jpn. **70**, 1417 (2001).
- ⁴⁹F. De Martini, G. Giuliani, and P. Mataloni, Phys. Rev. Lett. **35**, 1464 (1975).
- ⁵⁰K. Vogler, Phys. Status Solidi B **107**, 195 (1981).
- ⁵¹M. Casalboni, R. Francini, U. M. Grassano, and R. Pizzoferrato, Phys. Status Solidi B **117**, 493 (1983).
- ⁵²H. Hanzawa, Y. Mori, and H. Ohkura, Radiat. Eff. Defects Solids **119-121**, 791 (1991).
- ⁵³V. Hizhnyakov, Phys. Status Solidi B **114**, 721 (1982).
- ⁵⁴S. Muramatsu, J. Phys. Soc. Jpn. **6**, 1078 (1993).
- ⁵⁵Y. Kayanuma, Y. Mori, and H. Ohkura, J. Lumin. **38**, 139 (1987).

- ⁵⁶Y. Kayanuma, J. Phys. Soc. Jpn. **57**, 292 (1988).
- ⁵⁷M. Hama and M. Aihara, Phys. Rev. B **38**, 1221 (1988).
- ⁵⁸U. M. Grassano, G. Margaritondo, and R. Rosei, Phys. Rev. B **8**, 3319 (1970).
- ⁵⁹T. Iida, K. Kurata, and S. Muramatsu, J. Phys. Chem. Solids **33**, 1225 (1972).
- ⁶⁰Y. Kayanuma and K. Nasu, Solid State Commun. **27**, 1371 (1978).